Nanoscale

Accepted Manuscript

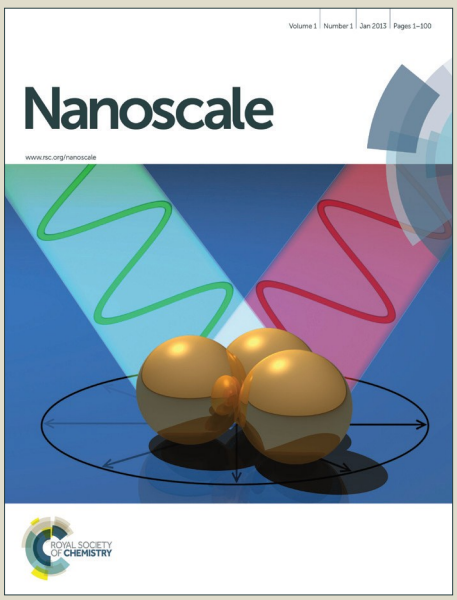

ROYAL SOCIETY OF CHEMISTRY

www.rsc.org/nanoscale

Journal Name

COMMUNICATION

Conductive Polymer-Mediated 2D and 3D Arrays of Mn_3O_4 Nanoblocks and Mesoporous Conductive Polymers as Their Replica

Received 00th January 20xx,
Accepted 00th January 20xx

DOI: 10.1039/x0xx00000x

www.rsc.org/

Yoshitaka Nakagawa, Hiroyuki Kageyama, Riho Matsumoto, Yuya Oaki and Hiroaki Imai*

Orientation-controlled 2D and 3D microarrays of Mn_3O_4 nanocuboids that were mediated by a conductive polymer were fabricated by evaporation-induced self-assembly of the oxide nanoblocks and subsequent polymerization of pyrrole in the interparticle spaces. Free-standing mesoporous polypyrrole (PPy) having chain- and square-grid-like nanovoid arrays were obtained as replicas of the composite assemblies by dissolving the oxide nanoblocks. The PPy-mediated manganese oxide arrays exhibited stable electrochemical performance as an ultrathin anode of a lithium-ion secondary battery.

Introduction

A wide variety of nanoscale crystals, such as nanospheres, nanorods, and nanosheets, have been produced as building blocks of hierarchical architectures.[1-4] The well-ordered arrangements of the monodisperse nanocrystals were formed from the dispersion through an evaporation-induced assembly process.[5-7] Notably, cube-shaped nanocrystals that are covered with amphiphilic molecules tend to assemble in the same crystallographic direction like a single crystal.[8-13] Recently, 1D, 2D, and 3D microarrays have been achieved by controlling the direction and dimension of the self-assembly of rectangular nanoblocks.[14,15] The well-aligned ensembles of inorganic nanocrystals often exhibit interesting collective properties that are different from those displayed by individual nanocrystals and bulky large crystals.[16,17] Moreover, a combination of the inorganic microarrays and organic polymers could provide fascinating functions. However, fabrication of the composite structures has not been reported. In the current study, we achieved 2D and 3D arrays of metal oxide nanoblocks mediated by a conductive polymer (Scheme 1).

The self-assembled nanospheres have been used as a template to produce elaborate porous replicas. Several replicas with hierarchical architectures and periodic macropores were fabricated by the introduction of polymers, oxides, or metals into the interparticle spaces and subsequent removal of the templates.[18-23] However, the size of the ordered voids prepared in the previous works was larger than several hundreds of nanometers.[18-23] The highly ordered arrays consisting of rectangular nanoblocks are expected to be deformable templates for the fabrication of aligned voids several tens of nanometers in size. Here, we prepared nanovoid arrays of a conductive polymer using the well-ordered arrays of metal oxide nanoblocks. The mesoporous replicas were produced through dissolution of the nanoblocks from the ordered arrays combined with the polymer (Scheme 1).

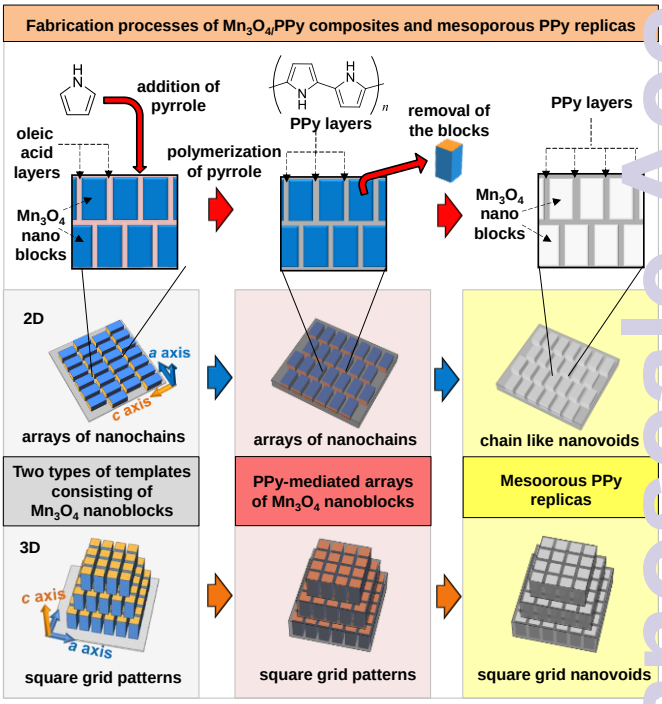

Scheme 1. Fabrication processes of ordered arrays of PPy-mediated Mn_3O_4 nanoblocks and their mesoporous PPy replicas having closed nanovoids.

Department of Applied Chemistry
Faculty of Science and Technology, Keio University
3-14-1 Hiyoshi, Kohoku-ku, Yokohama 223-8522 (Japan)
E-mail: hiroaki@applc.keio.ac.jp

In the current work, we focused on fabrication of the composite arrays consisting of polypyrrole (PPy)-mediated Mn_3O_4 nanocuboids. Manganese oxides have attracted much attention from a number of researchers as excellent electrode materials for manganese batteries, supercapacitors, and lithium-ion secondary batteries.[24-27] However, their low electrical conductivity and poor durability have interfered with their use as electrodes. Nanostructured electrodes have been widely expected to solve the problems described above because the nanoscale units can achieve short pathway distances for the transport of electrons and lithium ions.[28-31] Coating a conductive layer of carbon and polymers on the oxide surface was utilized to increase the electrical conductivity.[32-38] Here, control of the self-assembly process of Mn_3O_4 rectangular nanoblocks has been applied to the design of appropriate nanostructures for electrode active materials. Moreover, the Mn_3O_4 nanocrystals arranged on a substrate were coated with PPy on a nanometric scale through polymerization of pyrrole at the air–solid interphase.[36] The electrochemical characteristic of ultrathin electrodes consisting of the PPy-mediated arrays of the nanoblocks was evaluated as lithium-ion battery anodes.

Experimental Section

Synthesis of Mn_3O_4 rectangular nanoblocks. We prepared truncated Mn_3O_4 nanocuboids through a liquid–liquid two-phase (water and toluene) solvothermal method.[15] 0.60 mmol manganese(II) chloride and 35wt% hydrogen peroxide (4 cm^3) were dissolved in 31 cm^3 of water in a 100 cm^3 Teflon container. Oleic acid (3.97 mmol) and *tert*-butylamine (2.31 mmol) were added into 30 cm^3 toluene. The organic mixture was added to the Teflon container without stirring. At this time, oxygen gas was generated through decomposition of hydrogen peroxide. When the generation of oxygen gas roughly stopped, the Teflon container was put into a stainless steel autoclave. The autoclave was heated at 115°C for 12 h. After the reaction, the resultant dark brown liquid on the aqueous phase was transferred into a glass vial. A copper grid covered with a collodion film was placed on a piece of filter paper. A drop of the resultant dispersion was placed on the grid. After the excess medium of the dispersion was absorbed by the filter paper, the nanoblocks were deposited on the grid. Morphologies of nanocrystals were characterized by the transmission electron microscopy (TEM), high-resolution TEM (HRTEM), and fast Fourier transform (FFT) profiles using an FEI Tecnai-F20. Resultant dispersion and the equal amount of ethanol were mixed and then centrifuged at 13500 rpm for 5 min. The precipitates were used for the powder X-ray diffraction (XRD) measurement (Rigaku MiniFlex II).

Fabrication and characterization of ordered arrays consisting of Mn_3O_4 rectangular nanoblocks. The resultant dispersion of Mn_3O_4 nanoblocks was centrifuged at 13500 rpm for 5 min. The precipitates were redispersed into a hexane–toluene mixture (1 : 1 in volume) or toluene in a 6 cm^3 vial by ultrasonication for 30 min. The volume of the dispersions was 0.5 cm^3. The particle concentration was adjusted to 2.8×10^{-1} g/dm^3 (2D arrays) or 5.6×10^{-1} g/dm^3 (3D arrays). A silicon substrate (7 mm × 16 mm) treated by acetone with ultrasonication for 30 min was put in the dispersion in the vial. The dispersion spread on the substrate by its surface tensi The dispersion medium was evaporated at room temperature When the drying was completed, the morphologies o products were observed via the scanning electron microscop (SEM) using an FEI-Sirion.

Fabrication and characterization of PPy-mediated arrays of Mn_3O_4 nanoblocks and their porous PPy replicas. The powde of 240 mg iron(III) nitrate nonahydrate ($Fe(NO_3)_3 \cdot 9H_2O$), the neat liquid of 1 cm^3 pyrrole (C_4H_5N), and the ordered arrays o Mn_3O_4 nanoblocks deposited on the substrate were separately placed in a glass bottle. The glass bottle was covered with a container slightly larger than the bottle to prevent leak o pyrrole vapor. After sealing the sample bottle and containe the container were heated at 60˚C for 3 h. After the reactio the color of the walls of the sample bottle and the substrat changed to black. PPy-mediated arrays of Mn_3O_4 nanoblock formed on the substrate were peeled off by immersing black substrate in 0.5 cm^3 ethanol under ultrasonication for 10 min. Porous PPy films were fabricated by immersing the bl substrate in 0.5 cm^3 hydrochloric acid (dilute HCl, 2 mol/dm^3) under ultrasonication for 1 h. A copper grid was immerse the dispersion of PPy films. After pulling out the grid from th dispersion, the excess liquid adhering to the grid was absorbed by a filter paper. Morphologies and composition of th products deposited on the grid were characterized by TE with Energy-dispersive X-ray (EDX) analysis. Fourier transform infrared (FTIR) spectra were obtained by a Jasco FT/IR-420 Commercial PPy powder (Aldrich) was used as a reference.

Electrochemical characterization of ordered arrays of Mn_3O_4 nanoblocks and PPy-mediated arrays of Mn_3O_4 nanoblocks. The electrochemical performance was measured with beaker-type three-electrode cell. The working electrode was ordered arrays of Mn_3O_4 nanoblocks or PPy-mediated arrays o Mn_3O_4 fabricated on a copper substrate. A lithium metal was used for the counter and reference electrodes on a cop mesh. 1 mol/dm^3 of $LiClO_4$ in ethylene carbonate and diethy carbonate (1/1 volume) was used as the electrolyte. The cell was assembled in an argon-filled glove box. Discharge–charg measurements were performed in a potential range betwee 0.1 and 3.0 V vs. Li/Li^+ at room temperature. The cur density for the charge and discharge reactions was increase from 0.25 C to 10 C (1 C = 117 mA/g).

Results and Discussion

Truncated nanocuboids obtained by the two-phas solvothermal method were assigned to tetragonal Mn_3O_4 b XRD analysis and HRTEM images as reported in our previou work (Figure S1).[15] The resultant anisotropic nanoblocks wer covered with oleic acid molecules. The typical width and length of the Mn_3O_4 nanocuboids synthesized under th standard condition were ~10 nm and ~20 nm, respectively. 2D ordered arrays of the Mn_3O_4 rectangular nanoblocks wer fabricated on a silicon substrate from a dispersion of the cuboids by evaporation of a mixed medium of toluene and hexane (1:1 in volume). The 2D ordered structures with the

faces parallel to the substrate were observed by SEM (Figure 1a and b). Adsorbed molecular layers ~3 nm thick existed between adjacent nanoblocks in the ordered arrays as we reported in our previous article.[15]

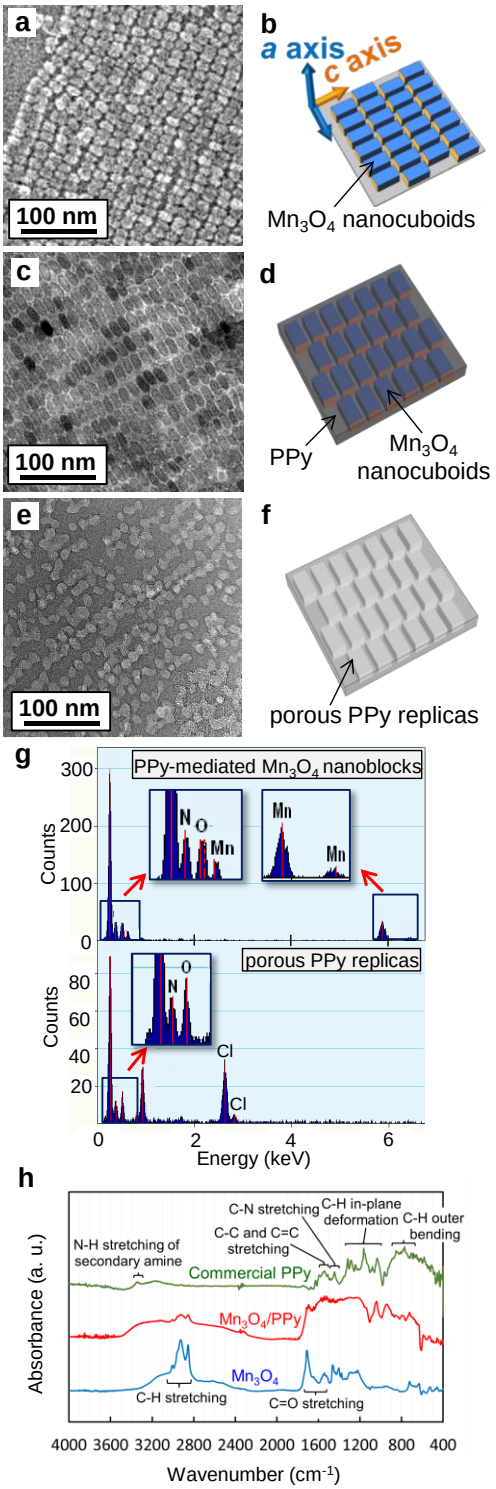

Figure 1. SEM image and schematic illustration of 2D arrays with *a* faces of Mn_3O_4 nanoblocks parallel to a substrate (a,b). TEM image and schematic illustration of PPy-mediated arrays of Mn_3O_4 nanoblocks (c,d). TEM image and schematic illustration of a PPy replica (e,f). EDX spectra (g) and FTIR spectra (h) of the PPy-mediated arrays of Mn_3O_4 nanoblocks and the PPy replica.

By the introduction of PPy into the interparticle spaces through polymerization of the vaporized pyrrole, the polymer-mediated 2D arrays were achieved. As reported in our previous work, amorphous PPy was formed around nanocrystals by the polymerization method (Figure S2).[36] We characterized the resultant films by TEM and EDX analysis. The ordered 2D arrays (Figure 1c and d) similar to the original structures (Figure 1a and b) were observed after the polymerization. Manganese from the oxide cuboids and nitrogen originating from PPy were detected in the composite films (Figure 1g, upper spectrum).

Figure 1h shows FTIR spectra of the Mn_3O_4 nanoblock arrays before and after PPy coating. Specific absorption peaks due to PPy in FTIR spectra indicate the presence of the polymer in the composite samples.[39] Thus, the 2D ordered arrays of Mn_3O_4 nanocuboids were mediated by PPy. Moreover, the absorption bands in 1500–1800 and 2800–3000 cm^{-1} indicate the existence of oleic acid in the nanoblock arrays even after the PPy coating. As shown in Figure 1h, PPy signals assigned to PPy in the composites are observed to be highly broadened by the hybridization. This indicates that the framework of PPy is strongly interacted with alkyl chains of oleic acid covering the nanoblock surface. The Py monomer penetrated into the interparticular layer and then polymerized among the nanoblocks.

After the Mn_3O_4/PPy composite films were immersed in dilute HCl solution, the 2D arrays remained in the films as shown in TEM images (Figure 1e and f). However, manganese was not detected in the films by EDX analysis (Figure 1g, lower spectrum). Therefore, the porous structures of PPy consisting of chain-like nanoscale voids were formed through dissolution of the Mn_3O_4 nanoblocks from the composites.

After the dissolution of Mn_3O_4 nanoblocks, we detected chlorine and oxygen that originated from residual HCl and oleic acid in the PPy films, respectively.

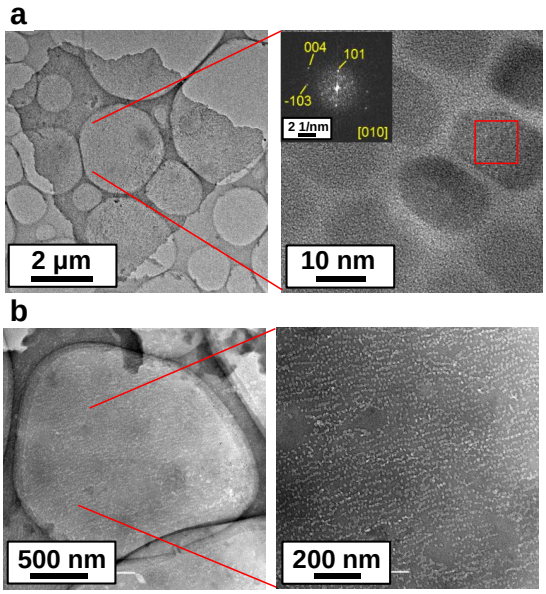

Figure 2. TEM and HRTEM image of self-standing PPy-mediated arrays of Mn_3O_4 nanoblocks and FFT pattern corresponding to the lattice fringes of a Mn_3O_4 nanoblock (red square region) (a). TEM images of a PPy replica film (b).

Self-standing films of Mn_3O_4 nanoblocks/PPy composites and porous PPy replicas were obtained by removal of the support substrates (Figure 2a and b). The crystalline phase of nanoblocks remained unaltered after the polymerization of pyrrole because the fast Fourier transform (FFT) patterns corresponding to the lattice fringes of the nanoblocks in the composite film were assigned to tetragonal Mn_3O_4 (inset of Figure 2a).

When toluene was used as a dispersion medium, 3D arrays with their *c* faces of Mn_3O_4 parallel to the substrate was obtained (Figure 3a and b).[15]

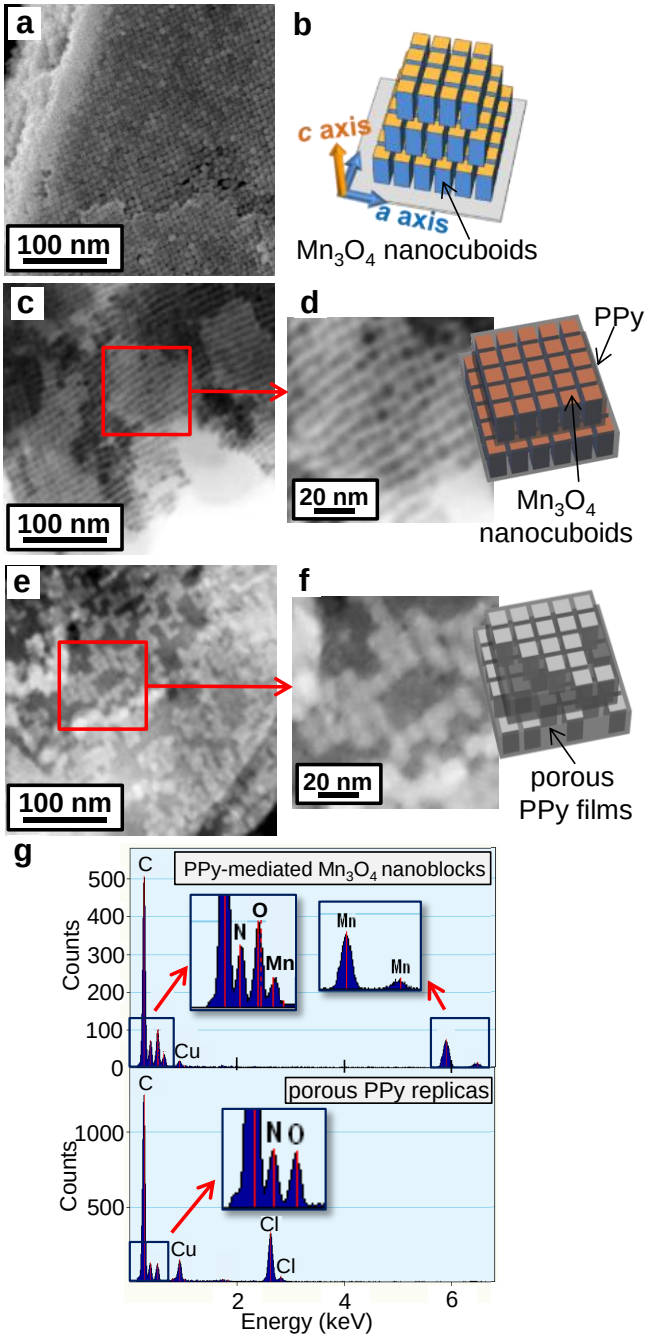

Figure 3. SEM image and schematic illustration of 3D arrays with *c* faces of Mn_3O_4 nanoblocks parallel to a substrate (a,b). Black/white inverted STEM images and schematic illustration of PPy-mediated arrays of Mn_3O_4 nanoblocks (c,d). Black/white inverted STEM images and schematic illustration of a PPy replica (e,f). EDX spectra of PPy-mediated arrays of Mn_3O_4 nanoblocks and the PPy replica (g).

We obtained square grid patterns consisting of Mn_3O_4 nanocuboids. The ordered PPy-mediated 3D arrays of Mn_3O_4 nanoblocks with the same square grid patterns were produced through introduction of the polymer into interparticle space (Figure 3c, d and g). The 3D PPy replicas having square-grid-like nanovoid arrays were produced by subsequent dissolution of the Mn_3O_4 nanocuboids (Figure 3e, f, and g).

The charge–discharge reactions with lithium ion were performed using the PPy-mediated 2D and 3D arrays of Mn_3O_4 nanoblocks fabricated on a copper substrate. The typical discharge curves of Mn_3O_4 were observed with the plateaus at 0.5 V (Figure 4a). The PPy-mediated 2D arrays of Mn_3O_4 nanoblocks showed improved specific capacity and stable cycle performance as compared to uncoated 2D arrays of Mn_3O_4 nanoblocks (Figure 4b).

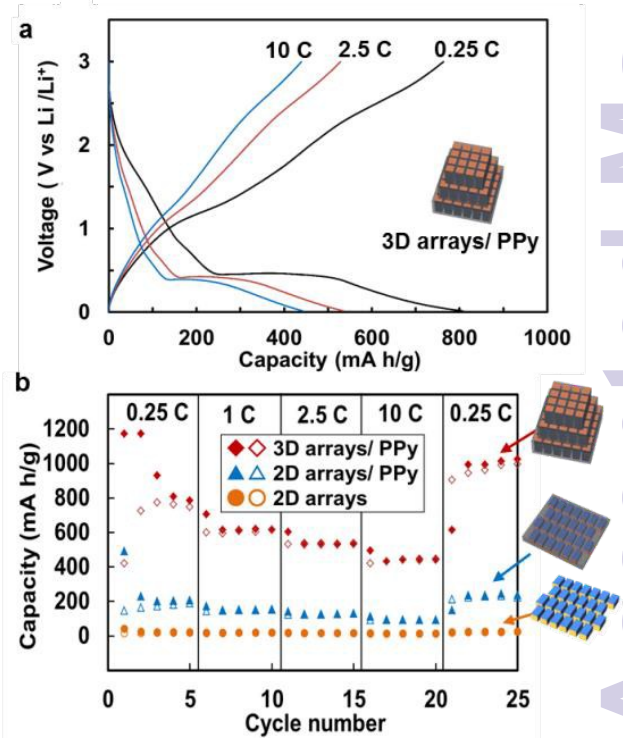

Figure 4. Charge and discharge curves of PPy-mediated 3D arrays of Mn_3O_4 nanoblocks fabricated on a copper substrate at the current density of 0.25 C at 4 th cycle, 2.5 C at 14 th cycle, and 10 C at 19 th cycle (1 C = 117 mA/g) (a). Charge and discharge capacities of 2D ordered arrays of Mn_3O_4 nanoblocks (circles), PPy-mediated 2D arrays of Mn_3O_4 nanoblocks (triangles), and PPy-mediated 3D arrays of Mn_3O_4 nanoblocks (squares) according to the cycle number (b). (Charge and discharge capacities are represented by non-filled and filled geometric symbols, respectively.)

The first and second discharge capacities of the ultrathin film electrode of 5- or 6-layered nanoblocks (3D arrays ~100 nm in thickness)/PPy composites were ~1170 mAh/g at the current density of 0.25 C. At a high current density (10 C), discharge and charge capacities were over 400 mAh/g. When the current density was turned back to 0.25 C, the ultrathin film electrode exhibited stable reversible capacities of around 900 mAh/g, which is close to the theoretical capacity for the fully reversible conversion reaction. The electrochemical capacities of the PPy-mediated 3D arrays of Mn_3O_4 nanoblocks are almost the same as that of Mn_3O_4 particles in the conventional system.[26,30] The improvement is ascribed to the

enhanced electron conductivity and stabilization of the nanocrystals on the conductive substrate by the presence of PPy that mediates Mn_3O_4 nanoblocks.

Conclusions

In this study, we fabricated 2D and 3D ordered arrays of Mn_3O_4 nanocuboids that were mediated by the conductive polymer by the polymerization of pyrrole in interparticle spaces. Self-standing mesoporous PPy replicas having chain- and square-grid-like nanovoid arrays were obtained from different types of PPy-mediated Mn_3O_4 nanoblocks. The dimension- and direction-controlled assembly of anisotropic nanoblocks is useful for the deformable template to regulate nanoscale morphologies of a wide variety of polymers. The ultrathin anodes of PPy-mediated 3D Mn_3O_4 nanoblock arrays exhibited stable electrochemical performance and excellent discharge–charge capacities for a lithium-ion battery.

Acknowledgments

This work was partially supported by the Advanced Low Carbon Technology Research and Development Program (ALCA) from Japan Science and Technology Agency (JST), a Grant-in-Aid for Challenging Exploratory Research (Grant 15K14129), and a Grant-in-Aid for Scientific Research (Grant 22107010) on Innovative Areas of "Fusion Materials: Creative Development of Materials and Exploration of Their Function through Molecular Control" (Area no. 2206) from the Ministry of Education, Culture, Sports, Science and Technology.

References

1 S. A. Harfenist, Z. L. Wang, M. M. Alvarez, I. Vezmar, R. L. Whetten, *J. Phys. Chem*. 1996, **100**, 13904.
2 K. An, N. Lee, J. Park, S. C. Kim, Y. Hwang, J.-G. Park, J.-Y. Kim, J.-H. Park, M. J. Han, J. Yu, T. Hyeon, *J. Am. Chem. Soc.* 2006, **128**, 9753.
3 T. Wang, J. Zhuang, J. Lynch, O. Chen, Z. Wang, X. Wang, D. LaMontagne, H. Wu, Z. Wang, Y. C. Cao, *Science* 2012, **338**, 358.
4 Y. C. Cao, *J. Am. Chem. Soc.* 2004, **126**, 7456.
5 T. P. Bigioni, X.-M. Lin, T. T. Nguyen, E. I. Corwin, T. A. Witten, H. M. Jaeger, *Nat. Mater.* 2006, **5**, 265.
6 M. Li, Y. Chen, N. Ji, D. Zeng, D.-L. Peng, *Mater. Chem. Phys*. 2014, **147**, 604.
7 T. Ming, X. Kou, H. Chen, T. Wang, H.-L. Tam, K.-W. Cheah, J.-Y. Chen, J. Wang, *Angew. Chem.* 2008, **120,** 9831; *Angew. Chem. Int. Ed.* 2008, **47**, 9685.
8 A. Demortière, P. Launois, N. Goubet, P.-A. Albouy, C. Petit, *J. Phys. Chem. B* 2008, **112**, 14583.
9 J. Zhang, H. Yang, K. Yang, J. Fang, S. Zou, Z. Luo, H. Wang, I.-T. Bae, D. Y. Jung, *Adv. Funct. Mater.* 2010, **20**, 3727.
10 T. Wang, X. Wang, D. LaMontagne, Z. Wang, Z. Wang, Y. C. Cao, *J. Am. Chem. Soc.* 2012, **134**, 18225.
11 C.-J. Chen, R.-K. Chiang, Y.-R. Jeng, *J. Phys. Chem. C* 2011, **115**, 18142.
12 C.-W. Liao, Y.-S. Lin, K. Chanda, Y.-F. Song, M. H. Huang, *J. Am. Chem. Soc.* 2013, **135**, 2684.
13 M. Agthe, E. Wetterskog, J. Mouzon, G. Salazar-Alvarez, L. Bergström, *CrystEngComm* 2014, **16**, 1443.
14 M. Rycenga, J. M. McLellan, Y. Xia, *Adv. Mater.* 2008, **20**, 2416.
15 Y. Nakagawa, H. Kageyama, Y. Oaki, H. Imai, *J. Am. Chem. Soc.* 2014, **136**, 3716.
16 S. Sun, C. B. Murray, D. Weller, L. Folks, A. Moser, *Science* 2000, **287**, 1989.
17 A. Martin, C. Schopf, A. Pescaglini, J. J. Wang, D. Iacopino, *Langmuir* 2014, **30**, 10206.
18 L.-Y. Yang, W.-B. Liau, *Macromol. Chem. Phys.* 2007, **208**, 99
19 K. Yoshino, S. B. Lee, S. Tatsuhara, Y. Kawagishi, M. Ozaki, A. A. Zakhidov, *Appl. Phys. Lett.* 1998, **73**, 3506.
20 F. Li, Z. Wang, N. S. Ergang, C. A. Fyfe, A. Stein, *Langmuir* 2007, **23**, 3996.
21 G. Guan, R. Zapf, G. Kolb, Y. Men, V. Hessel, H. Loewe, J. Ye, R. Zentel, *Chem. Commun.* 2007, 260.
22 N. R. Denny, S. E. Han, D. J. Norris, A. Stein, *Chem. Mater.* 2007, **19**, 4563.
23 S.-J. Huang, P.-Y. Chen, *Electrochim. Acta* 2013, **89**, 180.
24 K. Kordesh, M. Weissenbacher, *J. Power Sources* 1994, **51**, 6
25 B. Ammundsen, J. Paulsen, *Adv. Mater.* 2001, **13**, 943.
26 X. Fang, X. Lu, X. Guo, Y. Mao, Y.-S. Hu, J. Wang, Z. Wang, F. Wu, H. Liu, L. Chen, *Electrochem. Commun.* 2010, **12**, 1520.
27 J. Bhagwan, A. Sahoo, K. Lal Yadav, Y. Sharma, *Electrochim. Acta*, 2015, **174**, 992.
28 A. S. Aricò, P. G. Bruce, B. Scrosati, J.-M. Tarascon, W. Van Schalkwijk, *Nat. Mater.* 2005, **4**, 366.
29 J. Wang, N. Du, H. Wu, H. Zhang, J. Yu, D. Yang, *J. Power Sources* 2013, **222**, 32.
30 J. Gao, M. A. Lowe, H. D. Abruna, *Chem. Mater.* 2011, **23**, 3223.
31 H. Kageyama, Y. Oaki, H. Imai, *RSC Adv.* 2014, **4**, 44124.
32 Y. Piao, H. S. Kim, Y.-E. Sung, T. Hyeon, *Chem. Commun.* 2010, **46**, 118.
33 Z. Yang, J. Shen, N. Jayaprakash, L. A. Archer, *Energy Environ Sci.* 2012, **5**, 7025.
34 C. Wang, L. Yin, D. Xiang, Y. Qi, ACS *Appl. Mater. Interfaces* 2012, **4**, 1636.
35 B. Jang, M. Park, O. B. Chae, S. Park, Y. Kim, S. M. Oh, Y. Piao, T. Hyeon, *J. Am. Chem. Soc.* 2012, **134**, 15010.
36 R. Muramatsu, Y. Oaki, K. Kuwabara, K. Hayashi, H. Imai, *Chem. Commun.* 2014, **50**, 11840.
37 Z. Cai, L. Xu, M. Yan, C. Han, L. He, K. Mulonda Hercule, C. Niu, Z. Yuan, W. Xu, L.Qu, K. Zhao, L. Mai, *Nano Lett.* 2015, **15**, 738.
38 L. Zhang, K. Zhao, W. Xu, Y. Dong, R. Xia, F. Liu, L. He, Q. Wei, M. Yana, L. Mai, *Phys. Chem. Chem. Phys.* 2015, **17**, 7619.
39 K. Majid, R. Tabassum, A. F. Shah, S. Ahmad, M. L. Singla, *J. Mater. Sci. Mater. Electron.* 2009, **20**, 958.